OPEN ACCESS Freely available online

ISSN 2737-5323
Volume 2, Issue 3
https://www.iikii.com.sg/journal/AFM
Applied Functional Materials

Article

Study on Preparing β-Ga_2O_3 Films with Temperature-Controlled Buffer Layer by RF Magnetron Sputtering

Yi Liu, Tinglin He, and Sufen Wei *

School of Ocean Information Engineering, Jimei University, Xiamen 361021, China;
* Correspondence: weisufen@jmu.edu.cn; Tel.: +86-512-6190996

Received: Jul 29, 2022; **Accepted:** Aug 29, 2022; **Published:** Sep 30, 2022

Abstract: β-Ga_2O_3 thin films were prepared on (0006) sapphire substrates by RF magnetron sputtering. Under the conditions of sputtering power of 80 W, time of 10 min, and total flow rate of 40 sccm in oxygen and argon atmosphere (2.5 % oxygen ratio). Different preparation temperatures were used to conduct layering by temperature modulation. A homogenous β-Ga_2O_3 buffer layer was grown first, and then the second β-Ga_2O_3 film was grown on top of it. When the stratified sputtering of different temperature combinations was completed, high-temperature thermal annealing with the same parameters was performed. The effects on the structure, surface morphology, and optical properties of β-Ga_2O_3 thin films were compared and analyzed when using the preparation sequence of the homogenous buffer layer and the top layer at different temperatures after annealing. Finally, based on the stratified preparation temperature parameters, the optimal stratified temperature parameters were summarized.

Keywords: Gallium oxide, RF magnetron sputtering, Temperature, Buffer layer, Thermal annealing

1. Introduction

The monoclinic β-Ga_2O_3 has an ultra-wide bandgap and excellent thermal stability under normal pressure and temperature conditions [1–4]. Hence, it has advantages of applications in the areas of solar-blind UV photodetectors [3–7], gas sensors [8], solar cells [9], photocatalysts [10], phosphors [11], and next-generation power electronic devices [12–15]. The refined quality of β-Ga2O3 thin films is fundamental to realizing the development of devices and applications. Therefore, many epitaxial techniques for the generation of high-quality β-Ga_2O_3 have been reported. Among them, a commonly used method to produce the β-Ga_2O_3 films with comparatively low cost is RF magnetron sputtering [15–19]. However, because of the lattice mismatch and different coefficients of thermal expansion [20,21], high-quality β-Ga2O3 films were hard to grow directly on commonly used substrates such as sapphire and Silicon. It has been verified that the homo-buffer layers and annealing treatment can improve the polycrystalline quality of β-Ga_2O_3 films by Huang et al. [22], by employing the low sputtering temperature of 200 °C for generating the buffer layer, and a high sputtering temperature of 500 °C for generating the top layer. In this study, more combinations of different sputtering temperatures of lower and upper layers were conducted, and the influence of temperature combination and the annealing treatment on the morphology and optical properties of the β-Ga_2O_3 films were further investigated.

2. Materials and Methods

The (0006) sapphire substrate was sequentially cleaned with acetone, ethanol, and deionized water for 10 min to remove surface contamination and native oxides. The Ga_2O_3 films were deposited by RF magnetron sputtering with a Ga_2O_3 ceramic target with a purity of 99.99 % by a temperature-controlled layered preparation method. The bottom Ga_2O_3 buffer layer was first grown by sputtering on the sapphire substrate, and then the top Ga_2O_3 thin film was sputtered on the buffer layer. There were 6 samples in total, named Sample 1 to Sample 6. For the six samples, Tab1e 1 shows the sputtering parameters of the buffer and the top layers. The six samples after sputtering at different temperatures are as follows. (Sample 1) bottom room temperature and top 500 °C; (Sample 2) bottom 100 °C and top 500 °C; (Sample 3) bottom 200 °C and top 500 °C; (Sample 4) bottom 300 °C and top 500 °C; (Sample 5) bottom 400 °C and top 500 °C; (Sample 6): bottom 500 °C and top 200 °C. After sputtering, six samples were annealed with the same parameters. The annealing temperature was 800 °C and the annealing time was 2 hours. The annealing atmosphere was pure N_2, and the gas flow was 200 cc/min.

Table 1. Sputtering parameters of the buffer layer and the top layer.

	Sputtering temperature: buffer/top (°C/°C)	Sputtering power (w)	Flow ratio Ar2： O2	Base pressure (Pa)	Working pressure (Pa)	Duration of sputtering: buffer/top (min/min)
Sample 1	RT/500	80	39： 1	5·10E-4	0.8	10/10
Sample 2	100/500	80	39： 1	5·10E-4	0.8	10/10
Sample 3	200/500	80	39： 1	5·10E-4	0.8	10/10
Sample 4	300/500	80	39： 1	5·10E-4	0.8	10/10
Sample 5	400/500	80	39： 1	5·10E-4	0.8	10/10
Sample 6	500/200	80	39： 1	5·10E-4	0.8	10/10

The phase and composition of the samples were investigated by XRD (Malvern Panalytical EMPYREAN SERIES 3) in a scan range of 10º to 80º using a sampling pitch and preset time of 0.02º and 0.24 s, respectively. Cu–Ka radiation with a wavelength of 15.406 nm was operated at a voltage of 40 kV. The surface morphologies were analyzed by FESEM (Carl Zeiss/GeminiSEM300). The optical transmittance properties of the films were investigated using a UV–visible spectrophotometer (U-3900 Hitachi).

3. Results and discussion

After being grown and annealed, the XRD patterns of the six samples were compared in Fig. 1 with the standard powder diffraction files of PDF# 43-1013. Annealing promoted the conversion of Ga_2O_3 from the amorphous to the polycrystalline and the single crystal. In addition to the diffraction peak of the (0006) sapphire substrate, which was observed at 42.5° on the film, three distinct diffraction peaks located at around 18.7°, 38.2°, and 59.1° were observed in the XRD patterns of the Ga_2O_3 films. These diffraction peaks were respectively assigned to the ($\bar{2}01$), ($\bar{4}02$) and ($\bar{6}03$) planes of monoclinic β-Ga_2O_3, which indicated that the films on (0006) sapphire at various temperatures were pure β-Ga_2O_3 with the preferred orientation of {$\bar{2}01$}. Sample 6 showed the strongest diffraction intensities of the {$\bar{2}01$} phases of β-Ga_2O_3. In addition to the {$\bar{2}01$} which was a dominated orientation of β-Ga_2O_3, other β-Ga_2O_3 peaks became visible after annealing. These peaks belonged to the (400), (002), and (512) phases of β-Ga_2O_3. However, the intensities of these three diffraction peaks were much lower than those of the ($\bar{2}01$) and ($\bar{4}02$) diffraction peaks. Sample 6's diffraction intensity of the 2θ value of the ($\bar{2}01$) peak was the highest. Table. 2 lists the full width at half-maximum (FWHM) of the ($\bar{2}01$) peak and grain size obtained from the XRD patterns for the six samples after annealing. The result in Table 2 shows that the optimal temperature was 500 °C for the buffer layer and 200 °C for the top layer (Sample 6). The second best temperature was 200 °C for the buffer layer and 500 °C for the top layer (Sample 3). The third best temperature combination was room temperature for the buffer layer and 500 °C for the top layer (Sample 1).

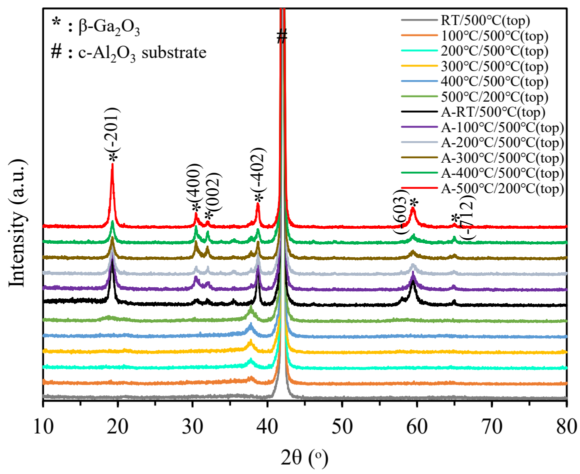

Fig. 1. XRD patterns of the six samples as-grown and after annealing, in comparison with ICDD file PDF# 43-1013 for β-Ga_2O_3. β-Ga_2O_3 is marked with an asterisk, and sapphire is marked with a hashtag.

Table 2. Sputtering parameters of the buffer layer and the top layer.

	Sputtering temperature: buffer/top (°C/°C)	FWHM (°)	grain size (nm)
Sample 1	A-RT/500	0.54	14.8
Sample 2	A-100/500	0.61	13.1
Sample 3	A-200/500	0.41	20.32
Sample 4	A-300/500	0.63	12.7
Sample 5	A-400/500	0.66	12.1
Sample 6	A-500/200	0.40	20.81

To explore the changes in surface morphology and roughness more clearly, the FESEM-examined surface morphologies of the β-Ga_2O_3 films after annealing were obtained (Figs. 2 (a)-(f)). The FESEM top view presents the grains of Samples 3 and 6 to be the most obvious and angular with the most uniform distribution. The grain sizes were also the largest, indicating the improvement of film crystalline quality. This result was consistent with the XRD results.

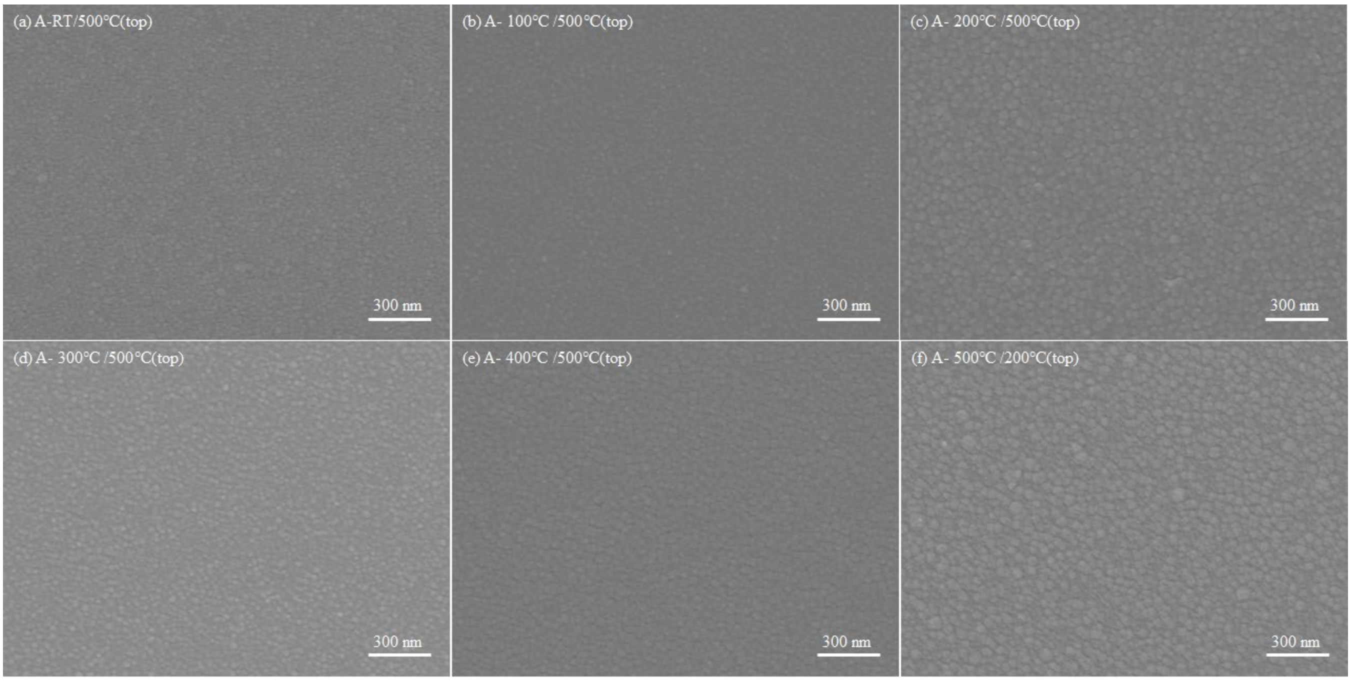

Fig. 2. SEM top images of Ga2O3 films after annealing.

The transmittance spectra in the wavelength range of 280–800 nm for the annealed β-Ga_2O_3 are shown in Fig.. 3. In the wavelength range of 280–800 nm, all six samples showed high average transmittance of 79.9% to 85.19 % (including the substrates). Table 3 shows the average transmittance of the six films with buffer layers after being annealed in different wavelengths. Figure 3 and Table 3 depict that the average transmittances of Samples 3 and 6 were slightly higher than the other samples in the band of 280–315 nm due to the better crystallinity and good uniformity of the films. This result of transmission is consistent with those of XRD and SEM.

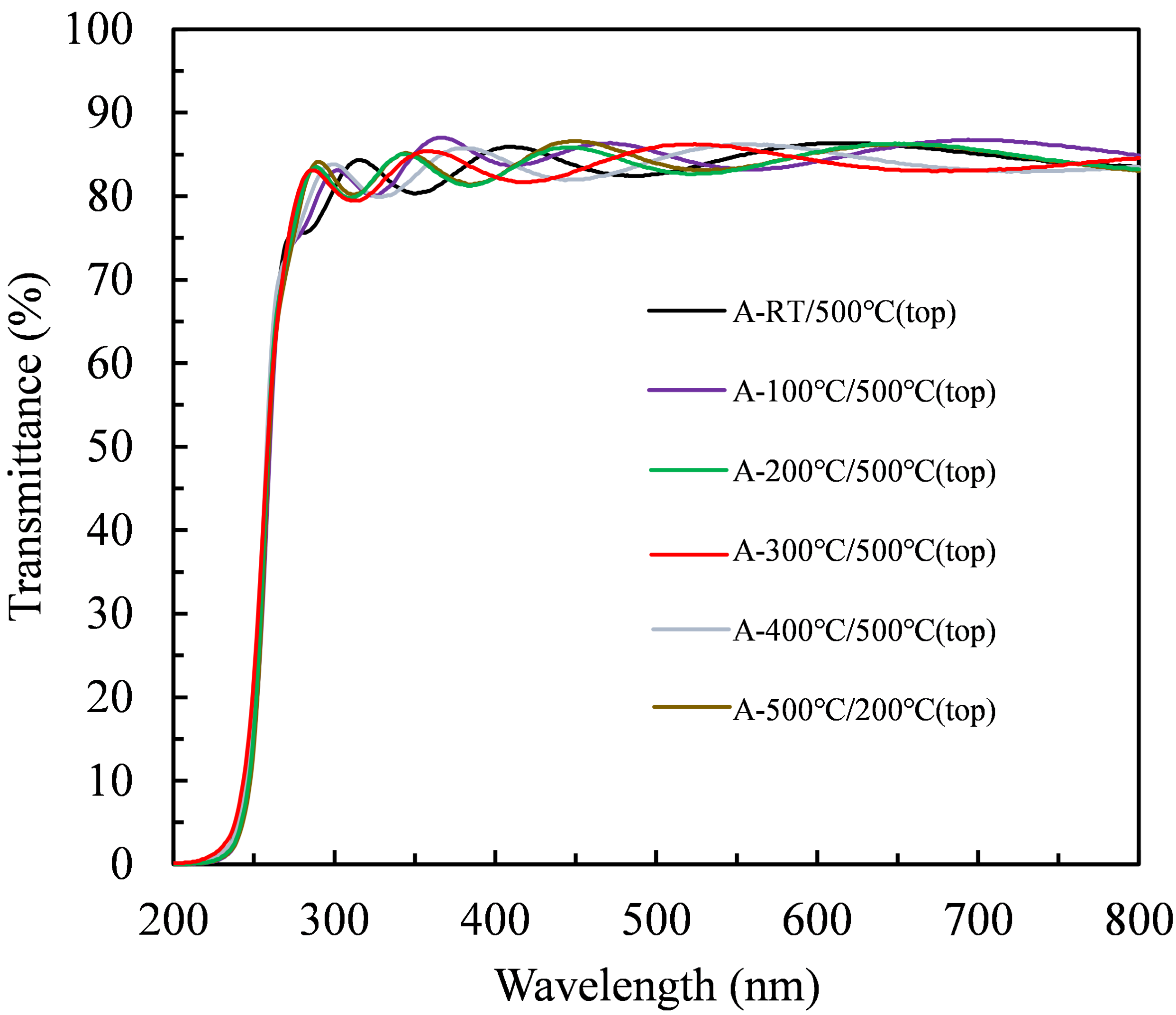

Fig. 2. Transmission spectra of the six samples after annealing.

Table 3. Average optical transmittance of six films with buffer layers after annealing in different wavelength bands.

	Sputtering temperature: buffer/top (°C/°C)	Average optical transmittance			
		200~280 (nm)	280~315 (nm)	315~400 (nm)	400~800 (nm)
Sample 1	RT/500	23.98	79.90	82.57	84.65
Sample 2	100/500	22.56	80.88	84.41	85.19
Sample 3	200/500	22.51	81.87	84.13	84.98
Sample 4	300/500	22.62	81.79	83.73	84.12

Table 3. *cont.*

Sample 5	400/500	23.57	81.44	82.69	84.57
Sample 6	500/200	22.74	81.99	83.96	84.77

The result also verified that the crystallization quality of Sample 6 was better than that of Sample 3. This is because the higher temperature was equivalent to sputtering deposition of the buffer layer during the buffer layer sputtering while annealing it at 500 °C, which promotes the crystallization quality of the buffer layer. On top of the better buffer layer, sputtering to deposit a gallium oxide film enbahces the quality of the overall film.

4. Conclusions

By employing RF magnetron sputtering, an improved method of double layer sputtering with different temperature control was presented in this study. The combinations of different sputtering temperatures of the buffer and the top layers was investigated with the influence of the temperature combinations on the properties of Ga_2O_3 films. After annealing, the β-Ga_2O_3 film with 500 °C sputtering at the bottom and 200 °C sputtering at the top had the smallest FWHM, the largest grain size, and the highest transmission, manifesting the optimal crystalline quality.

Author Contributions: Yi Liu carried out the experiments and analyzed the data and measurements; Tinglin He analyzed the data and measurements; Sufen Wei designed the experimental and test schemes, organized the data, and wrote the paper.

Funding: This work was supported by the Foreign Cooperation Project of Fujian Provincial Department of Science and Technology (Grant No. 2020I0022), the Provincial Natural Science Foundation of Fujian, China (Grant No. 2020J05150), and the Research Foundation of Jimei University (ZQ2019020).

Conflicts of Interest: The authors declare that they have no known competing financial interests or personal relationships that could have influenced the work reported in this paper.

References

1. Pearton, S.; Yang, J.C.; Cary, IV PH; Ren, F.; Kim, J.Y.; Tadjer, M.J.; et al. A review of Ga2O3 materials, processing, and devices. *Appl. Phys. Rev*. **2018**, *5*: 011301-1-56.
2. Litimein, F.; Rached, D.; Khenata, R.; Baltache, H. FPLAPW study of the structural, electronic, and optical properties of Ga2O3: Monoclinic and hexagonal phases. *J. Alloys Compd*. **2009**, *488*: 148–156.
3. Machon, D.; McMillan, P.F.; Xu, B.; Dong, J.J. High-pressure study of the β-to-a transition in Ga2O3. *Phys. Rev. B* **2006**, *73*: 094125–1–9.
4. Zinkevich, M.; Aldinger, F. Thermodynamic Assessment of the Gallium-Oxygen System. *J. Am. Ceram. Soc* **2004**, *87*: 683–691.
5. Wang, S.L; Chen, K.; Zhao, H.; He, C.; Wu, C.; Guo, D.; et al. β-Ga2O3 nanorod arrays with high light-to-electron conversion for solar-blind deep ultraviolet photodetection. *RSC Adv*. **2019**, *9*: 6064–6069.
6. Xu, J.; Zheng, W.; Huang, F. Gallium oxide solar-blind ultraviolet photodetectors: a review. *J. Mater. Chem. C*. **2019**, *7*: 8753–8770.
7. Kalygina, V.M.; Almaev, A.V.; Novikov, V.A.; Petrova, Y.S. Solar-Blind UV Detectors Based on β-Ga2O3 Films. *SEMICONDUCTORS*. **2020**, *54*: 682–686.
8. Manandhar, S.; Battu, A.K.; Devaraj, A.; Shutthanandan, V.; Thevuthasan, S.; Ramana, C.V. Rapid Response High temperature oxygen Sensor Based on titanium Doped Gallium oxide. *Sci. Rep*. **2020**, *10*: 178–1–9.
9. García-Carrión, M.; Ramírez-Castellanos, J.; Nogales, E.; Méndez, B.; You, C.C; Karazhanov, S.; et al. Hybrid solar cells with β- and γ-gallium oxide nanoparticles. *Mater. Lett*. **2020**, *261*: 127088–1–4.
10. Lee, J.H.; Doan, T.A.; Park, Y.J.; Hoa, H.T.M.; Phuong, P.H.; Le Dung Tien; et al. Synthesis and Photocatalytic Activity of β-Ga2O3 Nanostructures for Decomposition of Formaldehyde under Deep Ultraviolet Irradiation. *Catal*. **2020**, *10*: 1105–1–9.
11. Liu, X.M.; Yu, C.C.; Li, C.X.; Lin. Comparative study of Ga2O3: Dy3+ phosphors prepared by three methods. *J Electrochem Soc*. **2007**; *154*: 86–91.
12. Harada, T.; Ito, S.; Tsukazaki, A. Electric dipole effect in PdCoO2/b-Ga2O3 Schottky diodes for high-temperature operation. *SCI. ADV*. **2019**, *5*: eaax5733–1–7.
13. Zhang, S.Y.; Liu, Z.; Liu, Y.Y.; Zhi, Y.S.; Li, P.G.; Wu, Z.P.; et al. Electrical Characterizations of Planar Ga2O3 Schottky Barrier Diodes. *MICROMACHINES-BASEL*. **2021**, *12*: 259–1–8.
14. Singh, R.; Lenka, T.R.; Panda, D.K.; Velpula, R.T.; Jain, B.; Bui, H.Q.T.; et al. The dawn of Ga2O3 HEMTs for high power electronics - A review. *Mat Sci Semicon Proc*. **2020**, *119*: 105216–1–16.

15. Higashiwaki, M.; Sasaki, K.; Murakami, H.; Kumagai, Y.; Koukitu, A.; Kuramata, A.; et al. Recent progress in Ga2O3 power devices. Semicond. *Sci. Technol*. **2016**, *31*: 034001-1-11.
16. MOBTAKERİ, S.; TÜZEMEN, E.Ş.; ÖZER, A.; GÜR, E. Characterization of gallium oxide/glass thin films grown by RF magnetron sputtering. *Cumhuriyet Sci. J*. **2020**; *41*: 929–937.
17. Hu1, H.D.; Liu, Y.C.; Han, G.Q.; Fang, C.Z.; Zhang, Y.F.; Liu, H.; et al. Effects of Post Annealing on Electrical Performance of Polycrystalline Ga2O3 Photodetector on Sapphire. *Nanoscale Res. Lett*. **2020**, *15*: 100–1–8.
18. Mobtakeri, S.; Akaltun, Y.; Ozer, A.; Kılıç, M.; Tüzemen, E.S.; Emre, G. Gallium oxide films deposition by RF magnetron sputtering; a detailed analysis on the effects of deposition pressure and sputtering power and annealing. *Ceram. Int*. **2021**, *47*: 1721–1727.
19. Wang, J.; Ye, L.J.; Wang, X.; Zhang, H.; Li, L.; Kong, C.Y.; Li, W.J. High transmittance β-Ga2O3 thin films deposited by magnetron sputtering and post-annealing for solar-blind ultraviolet photodetector. *J. Alloys Compd*. **2019**, *803*: 9–15.
20. Choi, K.H.; Kang, H.C. Structural and optical evolution of Ga2O3/glass thin films deposited by radio frequency magnetron sputtering. *Mater Lett*. **2014**, *123*:160–164.
21. Feng, X.J.; Li, Z.; Mi, W.; Ma, J. Effect of annealing on the properties of Ga2O3: Mg films prepared on α-Al2O3 (0001) by MOCVD. *Vacuum*. **2016**, *124*: 101–107.
22. Huang, J.; Li ,B.; Ma, Y.C.; Tang, K.; Huang, H.F. ; Hu, Y.; Zou, T.Y.; et al. Effect of Homo-buffer Layers on the Properties of Sputtering Deposited Ga2O3 Films. IOP Conference Series-Materials Science and Engineering, Proceedings of the INTERNATIONAL CONFERENCE ON SMART ENGINEERING MATERIALS (ICSEM 2018), ROMANIA, MAR 07-09.